JOURNAL OF THERMOPHYSICS AND HEAT TRANSFER
Vol. 8, No. 3, July–Sept. 1994

Quantifying Specular Approximations for Angular Scattering from Perfectly Conducting Random Rough Surfaces

Ralph A. Dimenna* and Richard O. Buckius†
University of Illinois, Urbana, Illinois 61801

Angular scattering predictions for perfectly conducting random rough surfaces are obtained from rigorous electromagnetic scattering solutions and quantitatively compared with predictions from approximate specular solutions. The theoretical formulation of the electromagnetic scattering solution based on the extinction theorem and the Fresnel and Kirchhoff approximations are presented. One-dimensional random rough surface profiles are generated for a broad range of correlation lengths, rms roughness, wavelengths, and incident angles, including grazing incident angles and surfaces which exhibit significant forward and backscattering. An angular criterion, based on a finite angular region surrounding the specular direction, is used to evaluate the accuracy of the approximations. Surface parameter domains for accurate scattering predictions by the Fresnel and Kirchhoff approximations are evaluated on an angular basis. The regions of validity of both approximations are quantified and these regions are beyond those previously reported.

Nomenclature

a, b	=	Kirchhoff approximation coefficients
E	=	error between exact and approximate solutions
$\boldsymbol{E}$	=	electric field intensity vector
F	=	electric field intensity derivative
G	=	Green's function
$\boldsymbol{H}$	=	magnetic field intensity vector
$H_n^{(1)}$	=	Hankel function of first kind of order n
I	=	intensity
i	=	unit imaginary number
$\hat{\boldsymbol{i}}, \hat{\boldsymbol{j}}, \hat{\boldsymbol{k}}$	=	unit vectors
K	=	surface density
$\boldsymbol{K}$	=	wave vector
k	=	wave vector component
L	=	magnetic field intensity derivative
L_x, L_y	=	surface lengths
N	=	number of surface points for numerical computations
$\hat{\boldsymbol{n}}$	=	surface outward normal vector
R	=	Fresnel reflection coefficient
r	=	scattering reflection function
$\boldsymbol{r}, \boldsymbol{R}$	=	position vectors
S	=	surface perimeter
x, y, z, x', z'	=	surface coordinates
γ	=	normalization constant
δ	=	dirac delta function
$\varepsilon, \varepsilon_0$	=	permittivity, permittivity of free space
ζ	=	surface profile
θ	=	angle of energy
λ	=	wavelength of incident energy
μ, μ_0	=	permeability, permeability of free space
ρ'', ρ'	=	bidirectional reflection function, directional reflectivity
σ	=	rms roughness
τ	=	surface correlation length
Φ	=	radiant power flow
Ω	=	solid angle
ω	=	circular frequency of radiation

Subscripts

approx	=	approximate solution
exact	=	exact solution
SR	=	specular reflection
s	=	scattered
TE	=	transverse electric polarization
TM	=	transverse magnetic polarization
x, y, z	=	coordinates
0	=	incident
ζ	=	surface interface
λ	=	spectral

Superscripts

$'$	=	directional
$''$	=	bidirectional
$>$	=	above

Received Aug. 5, 1993; revision received Dec. 27, 1993; accepted for publication Jan. 3, 1994.

*Graduate Research Assistant, Department of Mechanical and Industrial Engineering, 1206 West Green Street.

†Richard W. Kritzer Professor, Department of Mechanical and Industrial Engineering, 1206 West Green Street. Associate Fellow AIAA.

Introduction

PREDICTING the angular reflection of radiation from rough surfaces by exact and approximate methods is important in the analysis of interface radiative heat transfer properties. Electromagnetic theory predictions, based on the extinction theorem,[1] now provide rigorous solutions through recent advances in numerical methods.[2-5] The specular approximations, Kirchhoff and Fresnel, and other simplified methods of predicting radiative properties only approximate the scattering phenomena.[4,6-11] Since these approximations are computationally less expensive than the rigorous exact solutions, the range of validity of the approximations is of interest.[12-15]

The bidirectional reflection function for the surface is the radiation property of interest. From the bidirectional reflection function, the hemispherical radiative properties of reflection and emission are obtained.[16] As an example of the type of angular results obtained by these methods, Fig. 1 shows a comparison of three scattering predictions of the bidirectional reflection function at normal incidence angle, $\theta_0 = 0$ deg, vs scattering angle θ_s, for a perfectly conducting random rough surface described by a correlation length to wavelength τ/λ and a rms roughness to wavelength σ/λ. The exact solution is the prediction based on the extinction theorem. This result shows that both the Fresnel approximation

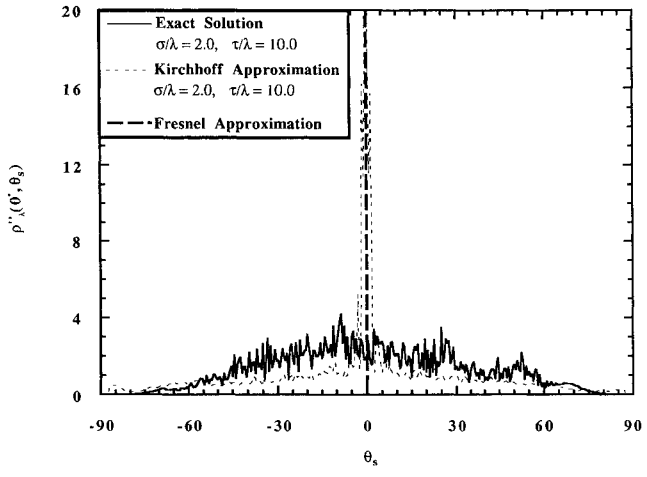

Fig. 1 Comparison of bidirectional reflection function predictions at $\theta_0 = 0$ deg vs θ_s for the exact solution, Kirchhoff approximation, and Fresnel approximation ($N = 2450$).

and the Kirchhoff approximation overpredict the scattered energy around the specular scattering angle, $\theta_s = 0$ deg. The Fresnel approximation predicts a single spike at the specular angle, whereas the Kirchhoff approximation, which is an extension of the Fresnel relations, predicts that the energy is scattered in a region very close to the specular angle. Conversely, the exact solution is relatively diffuse and has no dominant specular spike. If the surface scattering has a large degree of specular behavior, it can be well approximated by a specular approximation. Since the specular approximations are computationally less expensive than the exact solutions, the parameter domains for accurate predictions by these approximations are important to their usefulness.

Thorsos[14] performs a pointwise comparison of the Kirchhoff approximation with the exact solution over a range of scattering angles for surfaces with correlation length to wavelength ratios between $0.45 < \tau/\lambda < 4.75$, and roughness to wavelength ratios between $0.053 < \sigma/\lambda < 0.701$. From these comparisons, an angular criterion based on the scattering angle and a specified range of incident angles is given for the validity of the Kirchhoff approximation. The analysis does not, however, compare the Kirchhoff approximation with the exact solution for a large range of incident angles (i.e., restricted to nongrazing incident angles).

The conservation of energy criterion is used to verify that the specular approximations conserve energy. Previously, when the Kirchhoff approximation failed to predict conservation of energy, the approximation was considered invalid.[12] This criterion alone, however, does not determine whether the approximation is accurately predicting the angular scattering phenomena. The specular approximations can conserve energy and fail to accurately describe the angular scattering phenomena.

This current work defines an angular criterion for determining the accuracy of the specular approximations. Unlike Thorsos' comparison,[14] this work provides a comparison over a finite angular region to determine whether the approximations and the exact solutions are generally the same. A pointwise comparison yields a limited range of validity for the specular approximations, whereas a finite angular region comparison provides a broader region of usefulness. In addition, this work places no restrictions on either incident angles or surface parameters. Both grazing angles and a broad range of surfaces with significant forward and backscattering are analyzed.

Therefore, this work extends the previous work on the Kirchhoff approximation[12-15] for specular approximations. The Fresnel approximation is also analyzed as a specular approximation. The parameter domains of validity of both the Kirchhoff and Fresnel approximations for accurately predicting the angular scattering of electromagnetic energy are defined.

The following sections contain the formulation of the various scattering solutions and angular scattering results. This section contains the definition of the bidirectional reflection function that is used in the angular comparison of the rigorous solution with the approximations. The exact integral equation solution of Maxwell's equations is developed, along with the integral solution of the Kirchhoff approximation. The results and the angular criterion based on the region surrounding the specular angle are then developed. The Fresnel and Kirchhoff approximations are compared with exact solutions. Finally, the parameter domains of validity of the specular approximations are presented.

Analysis for Rough Interface Scattering

Interface Reflection Properties

Scattering processes characterize the change in directional and energy distribution of the wave incident upon an interface. The phenomena is expressed in terms of the incident power and the scattered power as the bidirectional reflection function. From the Poynting theorem relation,[17] the bidirectional reflection function is expressed as π times the ratio of the reflected radiant power per unit solid angle per unit area normal to the direction of reflection to the incident radiant power.[18] This function is

$$\rho''_\lambda(\theta_0, \theta_s) = \left(\frac{\pi}{\cos\theta_s}\frac{d\Phi_s}{d\Omega_s}\Big/\frac{d\Phi_0}{d\Omega_0}\right) \tag{1}$$

where θ_0 is the angle of incidence, θ_s is the reflection angle, and $d\Omega$ is the differential solid angle into which radiant power is incident or reflected. Hemispherical reflection from the surface is obtained by integrating Eq. (1) over all the scattering angles for a given incidence angle and assuming azimuthal symmetry. The other interface properties, emissivity, absorptivity, and transmissivity are obtained from Kirchhoff's law and conservation of energy on the surface.[16] The following sections formulate exact and approximate methods of obtaining Φ_s and Φ_0 for use in Eq. (1).

Electromagnetic Theory

Electromagnetic theory provides rigorous solutions for the scattering of incident waves from interfaces. The rough surface considered is shown in Fig. 2. The surface is one-dimensional, only varying in the x direction, so that scattering is considered in the plane of incidence. The surface interface is described by $z = \zeta(x)$ which separates a semi-infinite vacuum from a perfectly conducting material. The linearly polarized, monochromatic, plane electromagnetic incident wave strikes the surface at an incidence angle θ_0, with the z axis. The components of the incident and reflected wave vectors are, respectively

$$K_0 = k_0(\sin\theta_0, 0, -\cos\theta_0) \tag{2a}$$

$$K_s = k_0(\sin\theta_s, 0, \cos\theta_s) \tag{2b}$$

where $k_0 = 2\pi/\lambda$, and λ is the wavelength of the incident plane wave. Since only the plane of incidence is of interest, the electric field vector for TE polarization and the magnetic field vector for TM polarization have only $\hat{j}$ components, where $\hat{j}$ is the unit vector on the y axis (normal to the page in Fig. 2).

The incident electric vectors are

$$\boldsymbol{H}(x, z) = \hat{j}H_0 \exp\{ik_0(x\sin\theta_0 - z\cos\theta_0)\}$$

TM polarized (3a)

$$\boldsymbol{E}(x, z) = \hat{j}E_0 \exp\{ik_0(x\sin\theta_0 - z\cos\theta_0)\}$$

TE polarized (3b)

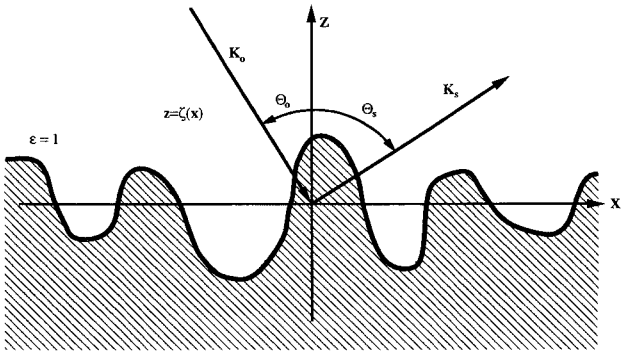

Fig. 2 Rough surface scattering geometry.

where E_0 and H_0 are the complex amplitudes of the incident wave. The time-dependence factor $\exp(-i\omega t)$ is suppressed throughout this presentation. The reflected field is now obtained by solving the corresponding Helmholtz equation.

The Helmholtz equation describing the magnetic and electric fields[17] is used to describe the fields above the surface described by Fig. 2. Both the $\boldsymbol{H}$ and $\boldsymbol{E}$ fields satisfy a continuity condition on the component tangent to the surface.[17] By using Maxwell's equations,[17] the following jump conditions are obtained:

$$H_y^>|_{z=\zeta(x)} = H(x) = K, \quad \text{TM polarization} \tag{4a}$$

$$E_y^>|_{z=\zeta(x)} = E(x) = 0, \quad \text{TE polarization} \tag{4b}$$

$$\left.\frac{\partial H_y^>}{\partial n}\right|_{z=\zeta(x)} = L(x) = 0, \quad \text{TM polarization} \tag{5a}$$

$$\left.\frac{\partial E_y^>}{\partial n}\right|_{z=\zeta(x)} = F(x) = i\omega\mu_0 K, \quad \text{TE polarization} \tag{5b}$$

where ω is in a vacuum, and μ_0 is the permeability of free space. The normal derivative in Eqs. (5) is given by

$$\frac{\partial}{\partial n} = (\hat{\boldsymbol{n}}\cdot\nabla) \tag{6}$$

The Helmholtz equation in two dimensions, with a line source is

$$\nabla^2 G_0 + k_0^2 G_0 = -4\pi\delta(x - x_0)\delta(z - z_0) \tag{7}$$

where G_0 is the two-dimensional Green's function. After a coordinate transformation, the two-dimensional Green's function is expressed in terms of the zeroth order Hankel function of the first kind[19] as

$$G_0(|\boldsymbol{r} - \boldsymbol{R}|) = i\pi H_0^{(1)}(k_0|\boldsymbol{r} - \boldsymbol{R}|) \tag{8}$$

The new coordinates are given by $\boldsymbol{r} = x\hat{\imath} + z\hat{\boldsymbol{k}}$ and $\boldsymbol{R} = x'\hat{\imath} + z'\hat{\boldsymbol{k}}$.

In order to obtain the scattered power in terms of the scattering angle θ_s, Eq. (8) is integrated over the volumetric vacuum above the surface. By use of Green's theorem, the volumetric integral of Eq. (7) is expressed as an integral over an arbitrary surface S. After substituting the Helmholtz equation[17] and Eq. (8), the volumetric integral is reduced, and the surface integral for TM polarization is expressed as

$$-4\pi H_y^>(x, z) = \int_S \left[H_y^>(x', z')\frac{\partial G_0(x, z, x', z')}{\partial n} - G_0(x, z, x', z')\frac{\partial H_y^>}{\partial n}\right] da' \tag{9}$$

For TE polarization, the surface integral is the same as Eq. (9) with E_y replacing H_y. Equation (9) is an integral over an arbitrary surface S, and da' is an arbitrary differential. Since the surface is arbitrary, the integral is taken over a surface at infinity added to an integral taken over the material surface. The integral over the surface at infinity is interpreted as the incident field.[1] In this way, Eq. (9) becomes

$$-4\pi H_y^>(x, z) = -4\pi H_y^>(x, z)_0 + \int_{S_\zeta}\left[H_y^>(x', z')\frac{\partial G_0(x, z, x', z')}{\partial n} - G_0(x, z, x', z')\frac{\partial H_y^>(x', z')}{\partial n}\right] da' \tag{10}$$

Again, the formulation for the TE polarization is the same with E_y replacing H_y. By substituting Eqs. (5), (6), and

$$da' = L_y\sqrt{1 + \zeta'(x)^2}\, dx' \tag{11}$$

into Eq. (10) and the analogous equation for TE polarization, the integral equations for the magnetic and electric fields are

$$H_y^>(x, z) = H_y^>(x)_0 + \frac{1}{4\pi}\int_{-\infty}^{\infty}\left\{H(x')\left[-\zeta'(x')\frac{\partial}{\partial x'} + \frac{\partial}{\partial z'}\right] G_0(x, z, x', z')|_{z'=\zeta(x')}\right\} dx' \tag{12a}$$

$$E_y^>(x)_0 = \frac{1}{4\pi}\int_{-\infty}^{\infty}[G_0(x, z, x', z')F(x')|_{z'=\zeta(x')}]\, dx' \tag{12b}$$

where G_0 is given by Eq. (9), and L_y is the length of the surface in the $\hat{\jmath}$ direction. The Hankel function in G_0 has a singularity and must be directly integrated by numerical computation.[2-4] Equations (12) are the integral equations governing surface scattering from a perfectly conducting surface. With the integral representation of G_0, Eqs. (12) provide the angular spectrums of the scattered fields. The total power scattered into the region above the material surface is calculated from the Poynting power theorem.[17] After evaluating the integral of the power theorem, the power scattered into any angle is

$$\frac{d\Phi_s}{d\theta_s} = \frac{L_y}{8\varepsilon_0\omega}\frac{k_0}{2\pi}|r_{TM}(\theta_s)|^2, \quad \text{TM polarization} \tag{13a}$$

$$\frac{d\Phi_s}{d\theta_s} = \frac{L_y}{8\mu_0\omega}\frac{k_0}{2\pi}|r_{TE}(\theta_s)|^2, \quad \text{TE polarization} \tag{13b}$$

where ε_0 is the permittivity of free space and the scattering reflection functions, $r_{TM}(\theta_s)$ and $r_{TE}(\theta_s)$, are given by

$$r_{TM}(\theta_s) = \int_{-\infty}^{\infty}\left(\exp\{-ik_0[x\sin\theta_s + \zeta(x)\cos\theta_s] \times \{ik_0[\zeta'(x)\sin\theta_s - \cos\theta_s]H(x)\}\right) dx \tag{14a}$$

$$r_{TE}(\theta_s) = \int_{-\infty}^{\infty} -F(x)\exp\{-ik_0[x\sin\theta_s + \zeta(x)\cos\theta_s]\}\, dx \tag{14b}$$

After evaluating the magnitude of the incident power flow with the Poynting power theorem, the result and Eqs. (13) are substituted into Eq. (1) to give the desired result for the polarized bidirectional reflection functions as

$$\rho''_{xTM}(\theta_0, \theta_s) = \frac{1}{8\pi}\frac{1}{L_x\cos\theta_s\cos\theta_0}|r_{TM}(\theta_s)|^2 \tag{15a}$$

$$\rho''_{xTE}(\theta_0, \theta_s) = \frac{1}{8\pi}\frac{1}{L_x\cos\theta_s\cos\theta_0}|r_{TE}(\theta_s)|^2 \tag{15b}$$

For unpolarized radiation, a simple average of Eqs. (15) is taken. The equations for bidirectional reflection can be integrated over the surface to obtain hemispherical reflection, which in the case of perfectly conducting surfaces, must equal 1.0.

Fresnel Approximation

When the geometric length scales of a rough surface are much smaller than the wavelength of the incident energy, the surface is considered optically smooth. The Fresnel approximation describes the bidirectional reflection functions by neglecting all roughness in surface profile. The Fresnel reflection coefficients, R_{TM} and R_{TE}, are a function of the dielectric properties of the surface, the incident angle of energy, and the polarization of the incident energy.[18] For a perfectly conducting surface considered here, the Fresnel approximation treats the surface as a plane, and all of the incident energy is reflected. Therefore, θ_s is equivalent to θ_0. The approximation assumes that all the incident energy is directed into a specular spike, which is represented by a dirac delta function at θ_s. The unpolarized result from Eqs. (15) from electromagnetic theory is compared with this Fresnel delta reflection function at $\theta_s = \theta_0$.

Kirchhoff Approximation

The Kirchhoff approximation is an extension of the Fresnel approximation that incorporates additional scattering phenomena. At every point on the surface, the scattered electric field $E(x)$, and magnetic field $H(x)$, and their derivatives $F(x)$ and $L(x)$, are approximated by the field that would exist on a plane tangent to the surface at that point.[7] By the nature of the approximation, it is most accurate when the radius of curvature of the surface roughness is large in comparison with wavelength, and breaks down as the radius of curvature approaches the order of the wavelength. The electric field and electric field derivative on the surface are approximated as[7]

$$E(x, z) = [1 + R_{TE}(x)]E_y^>(x, z)_0 \tag{16}$$

$$F(x, z) = \frac{\partial E(x, z)}{\partial n}\bigg|_{z=\zeta(x)} = ik_0 \cdot \hat{n}[1 - R_{TE}(x)]E_y^>(x, z)_0 \tag{17}$$

where $R_{TE}(x)$ is the Fresnel reflection coefficient at every surface position. The magnetic field and derivative are analogously developed

$$H(x, z) = [1 - R_{TM}(x)]H_y^>(x, z)_0 \tag{18}$$

$$L(x, z) = \frac{\partial H(x, z)}{\partial n}\bigg|_{z=\zeta(x)} = ik_0 \cdot \hat{n}[1 - R_{TM}(x)]H_y^>(x, z)_0 \tag{19}$$

Equations (16–19) are substituted into the Helmholtz equation on the surface and normalized with the analogous incident energy formulation to give an integral equation for the bidirectional reflection function as[7]

$$\rho''_\lambda(\theta_0, \theta_s) = \frac{1}{4L_x \cos\theta_0}\int_{-L_x}^{L_x} [a\zeta'(x) - b]\exp\{ik_0[(\sin\theta_0 - \sin\theta_s)x + (\cos\theta_0 + \cos\theta_s)\zeta(x)]\}\,dx \tag{20}$$

where a and b contain the Fresnel reflection coefficients and functions of the incident and scattering angles. For a perfectly conducting surface, however, all of the incident energy is reflected, so the coefficients, a and b, are reduced to functions of the incident and scattering angles.[7] Evaluating Eq. (20) with the assumptions that L_x is much larger than the wavelength of the incident energy and that the edges of the surface are fixed, yields the following result for the bidirectional reflection function[7]:

$$\rho''_\lambda(\theta_0, \theta_s) = \frac{1}{2L_x \cos\theta_0}\frac{1 + \cos(\theta_0 + \theta_s)}{\cos\theta_0 + \cos\theta_s} \times \int_{-L_x}^{L_x} \exp\{ik_0[(\sin\theta_0 - \sin\theta_s)x - (\cos\theta_0 + \cos\theta_s)\zeta(x)]\}\,dx \tag{21}$$

The bidirectional reflection function is independent of polarization for a perfectly conducting surface. This function is integrated over all the scattering angles for a given incident angle to obtain the hemispherical reflection function. Equation (21) is the result that is compared with the unpolarized result from Eqs. (15) from electromagnetic theory.

Numerical Implementation

The scattering equations given by both the electromagnetic theory formulation and the Kirchhoff approximation are solved numerically. For the resulting electromagnetic theory scattering equations, accurate solutions are obtained by using a quadrature scheme. The numerical method used is described in Refs. 2–6 and 20.

The integral equations are discretized over the interval of interest, L_x, so that the integrals are replaced with summations of N intervals. First, the infinite integral is converted to a finite one. Abscissas are constructed at equally spaced points along the finite L_x. With this discretization, the integral equation, Eq. (12) has a matrix form.[2,4,20] Assuming that $H(x)$ and $F(x)$ are slowly varying functions in x, allows the matrix element integrations to be replaced by summations. The matrix elements are provided by Maradudin et al.[2]

With the matrix elements, the unknowns $H(x)$ and $F(x)$ are determined. $H(x)$ and $F(x)$ are then used in Eqs. (14) to find the reflection function for each polarization. These integral functions are also discretized over an interval of $-L_x/2$ to $L_x/2$. These discretized expressions are solved and used in the bidirectional reflection function equations, Eqs. (15).[20]

All equations are programmed on a Cray Y-MP4/464 using LAPACK-b1 routines to solve for the unknowns, $H(x)$ and $F(x)$. The specific routines used are CGETRF and CGETRS, which factor the matrix into its LU decomposition and solve the matrix, respectively. Simple polynomial approximations[21] are used to obtain values of the Hankel functions within the matrix elements. Rough surfaces require averages of many surface realizations. The averages $\langle|r_{TM}(\theta_s)|^2\rangle$ and $\langle|r_{TE}(\theta_s)|^2\rangle$ are then used in the bidirectional reflection function Eqs. (15). Therefore, the scattering properties of a generic rough surface with given roughness and correlation parameters are determined.

For the Kirchhoff approximation, the integral equation for the bidirectional reflection function is also discretized. In this case, however, the integral has already been restricted to the surface integral. The Kirchhoff approximation is much easier to program than the system of equations for the electromagnetic theory solution. The surface matrices are eliminated in the Kirchhoff approximation and the computation time is significantly reduced. The summation portion of the Kirchhoff approximation is dependent on the surface and is averaged over a number of surface realizations as in the electromagnetic theory solution. The Kirchhoff approximation is also programmed on the Cray Y-MP4/464, although it can easily be solved on a workstation.

Results

Random Rough Surfaces

The random rough surfaces are described by a statistically homogeneous and isotropic process, $z = \zeta(x)$, with statistical properties as follows[2,4]:

1) Zero mean deviation from $z = 0$

$$\langle\zeta(x)\rangle = 0 \tag{22}$$

2) Root-mean-square roughness σ given by normal statistics

$$\sigma = [\langle \zeta(x)\zeta(x)\rangle]^{1/2} \tag{23}$$

3) τ defined by the width of a Gaussian correlation function $c(T)$, where T is the length over which the correlation diminishes by a factor of e, as

$$c(T) = (1/\sigma^2)\langle \zeta(x)\zeta(x + T)\rangle = \exp[-(T^2/\tau^2)] \tag{24}$$

A Monte Carlo method, which transforms a uniformly distributed sequence of random numbers between (0, 1) with the above statistics, is used to generate the surface profiles. This method is described and further developed in Refs. 2–6 and 9.

Each of the following results is averaged over 100 rough surface profiles. Each L_x is discretized into at most 2450 points in x, depending on the roughness of the surface. Surfaces that are more optically smooth do not require as many points as a surface which deviates significantly from x. Surface lengths are typically 100–200λ, depending on τ/λ. The surface length is made as long as possible to minimize the edge effects from the incident plane wave on the surface. For perfectly conducting surfaces considered here, all of the incident energy must be reflected. Therefore, the hemispherical reflection function for the surface must equal unity. All results presented conserve energy to within 0.1%.

Criteria for Directional Comparisons

Accurate approximations to electromagnetic scattering theory must characterize the distribution of scattered energy well. It is possible for the scattered energy to be conserved, yet the predicted directional distribution of the scattered energy could be inaccurate. For this reason, a directional criterion for assessing the accuracy of the Fresnel approximation and the Kirchhoff approximation is necessary. The conservation of energy criterion for assessing approximate solutions has been performed previously,[12] yet a directional comparison of the scattering phenomena is the goal of this work. Therefore, a directional criterion that compares the angular nature of the exact solution and the approximations is developed.

This criterion utilizes a finite angular region surrounding the specular scattering region, $\Delta\theta_{SR}$. The criterion is the difference in the energy predicted by the approximate solution and the exact solution relative to the energy predicted by the exact solution. When this ratio is less than a specific margin E, then the two predictions are in good agreement and the approximation is considered valid. The criterion is expressed as

$$\frac{\int_{\Delta\theta_{SR}} \left| I_{exact} \cos\theta_s - I_{approx} \cos\theta_s \right| d\theta_s}{\int_{\Delta\theta_{SR}} I_{exact} \cos\theta_s \, d\theta_s} < \mathfrak{E} \tag{25}$$

where $\Delta\theta_{SR}$ in Eq. (25) is the specified angular region surrounding the specular region, and I is the intensity distribution of the scattering. For this work, the angular regions are set to ±10 deg for the Kirchhoff approximation. For the Fresnel approximation, two angular regions of ±10 and ±5 deg are used. The criterion is valid for all surfaces, including nonperfectly conducting cases, although only perfectly conducting cases are considered here.

Directional Comparisons of Specular Engineering Approximations with Electromagnetic Theory

Figure 3 compares the Fresnel approximation with typical exact solutions. The bidirectional reflection function for the given incident angle, $\theta_0 = 15$ deg, is presented vs all θ_s for the approximation and two exact solutions. The Fresnel approximation is a specular spike at the scattering angle which mirrors the incident angle, in this case, $\theta_s = 15$ deg. All of the incident energy is contained within this specular spike. The Fresnel approximation for a given incident angle is the same regardless of the surface description because the approximation assumes that the surface is optically smooth.

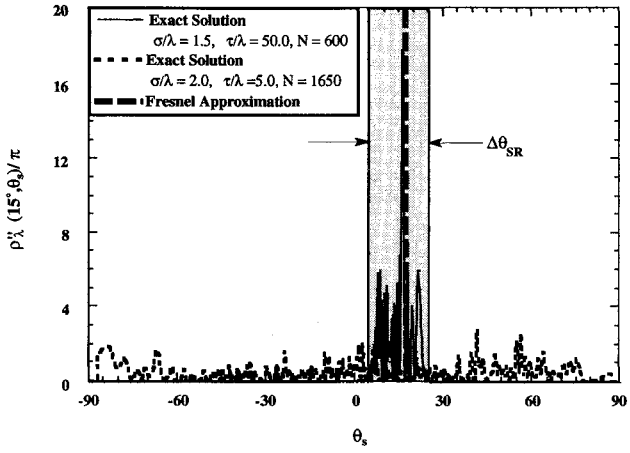

Fig. 3 Comparison of exact solutions with the Fresnel approximation for the bidirectional reflection function at $\theta_0 = 15$ deg vs θ_s for two surface profiles.

For surfaces that are very close to optically smooth, the exact solution predicts a reflection distribution that is very specular and surrounds the specular reflection angle, $\theta_s = \theta_0$. For surfaces that are not optically smooth, the exact solution predicts a more diffuse reflection distribution which deviates significantly from the specular spike. Figure 3 shows examples of these two limits in surface scattering. The angular region, $\Delta\theta_{SR}$, described previously, is used to describe the angular reflection of energy around the specular spike, which is the Fresnel approximation. The Fresnel approximation is considered valid [see criterion in Eq. (25)] if it does not overpredict the percentage of the exact reflected energy in the region described by $\Delta\theta_{SR}$. The angular region and the percent of energy reflected within the region described must be determined for each individual application. Typically, $\Delta\theta_{SR}$ ranges from ±5 to ±10 deg, and the Fresnel prediction of reflected energy in the region described by $\Delta\theta_{SR}$ differs from the exact solution in terms of the error, $\mathfrak{E}$, described in Eq. (25), by less than 5 or 10%. The exact solution for the surface described by a correlation length to wavelength ratio, $\tau/\lambda = 50.0$, and a rms roughness to wavelength ratio, $\sigma/\lambda = 1.5$, as shown in Fig. 3, is well approximated by the Fresnel solution since 99% of the reflected energy ($\mathfrak{E} = 0.01$) is contained within the region described by $\Delta\theta_{SR} = \pm 10$ deg. Conversely, the exact solution for the surface described by a correlation length, $\tau = 5.0\lambda$, and a rms roughness, $\sigma = 2.0\lambda$, as shown in Fig. 3, is not well approximated by the Fresnel solution.

If a surface is well approximated by the Fresnel solution for the desired angular and error criteria, then the computational cost to obtain the exact solution is not justified. The exact solution takes approximately 30 Mwords of memory and 2 h of CPU time to predict the averaged scattering from 100 surface profiles. The Fresnel approximation is made in seconds with simple computations. For many applications, the Fresnel solution is an adequate approximation to the exact solution found from electromagnetic theory. If an exact reflection distribution or specific magnitude of reflected energy at a certain θ_s is desired, then the exact solution must be used.

The Kirchhoff approximation has a larger region of validity than the Fresnel approximation. Similar to the exact solution, the Kirchhoff approximation predicts a reflected energy distribution which surrounds the specular spike, $\theta_s = \theta_0$. Again, the region of reflected energy is described by a specular angular region, $\Delta\theta_{SR}$. Since the Kirchhoff approximation is also a single scattering solution, it overpredicts the reflection in

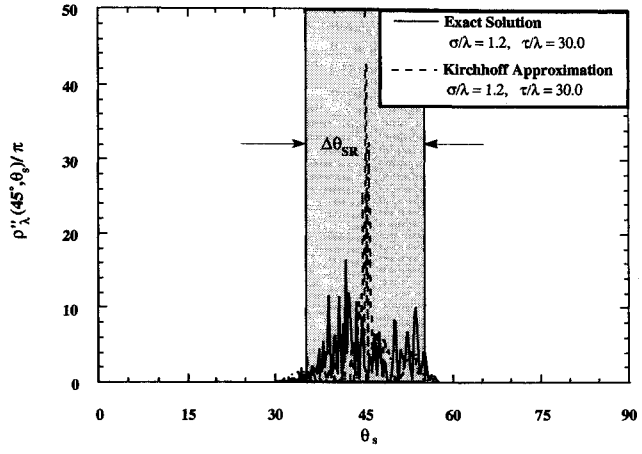

Fig. 4 Comparison of exact solution with the Kirchhoff approximation for the bidirectional reflection function at θ_0 = 0 deg vs θ_s (N = 1000).

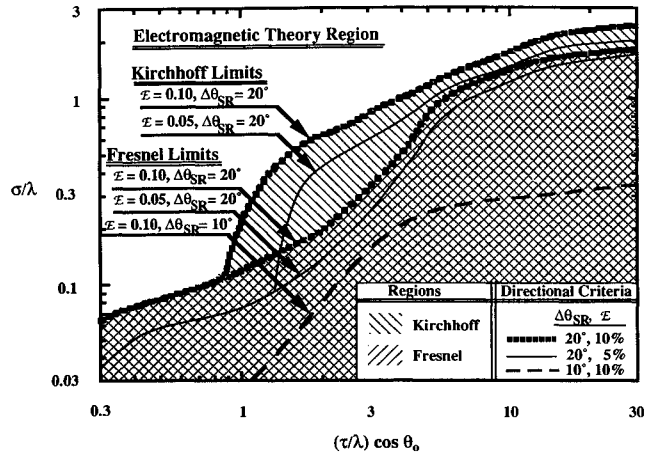

Fig. 5 Electromagnetic theory rough surface scattering domain plot with regions of validity for Kirchhoff and Fresnel approximations. $\mathcal{E}$ refers to energy difference between exact and approximate solutions in Eq. (25). $\Delta\theta_{SR}$ = ±5 or ±10 deg for all solutions.

the specular direction. Figure 4 shows a typical comparison of an exact solution and the Kirchhoff approximation. The bidirectional reflection function for a given incident angle, θ_0 = 45 deg, is presented for all θ_s. The same surface described by a correlation length to wavelength ratio, τ/λ = 30.0, and a rms roughness to wavelength ratio, σ/λ = 1.2, is used for both the exact solution and the Kirchhoff approximation. When the distribution of reflected energy predicted by the exact solution is within a specified percentage of the distribution of energy predicted by the Kirchhoff approximation, in a region described by $\Delta\theta_{SR}$, then the approximation is considered valid [see criterion in Eq. (25)]. Again, the angular region describing the region of reflected energy and the percentage of accuracy are $\Delta\theta_{SR}$ = ±5 or ±10 deg, and $\mathcal{E}$ < 5 or 10%, for the Kirchhoff solution to be an adequate approximation.

Figure 4 shows a typical Kirchhoff approximation which compares well with the exact solution for the same surface profile. Both the exact solution and the Kirchhoff approximation conserve energy to within 0.1%. For a reflection region described by $\Delta\theta_{SR}$ = ±10 deg, the Kirchhoff approximation is within 95% ($\mathcal{E}$ = 0.05) of the exact solution. If an exact distribution of reflected energy is needed, then the exact solution must be used. However, if only the approximate distribution is needed, then the Kirchhoff approximation is a computationally less expensive method of predicting the scattering. For 100 realizations of a given surface, the Kirchhoff approximation requires approximately 0.5 Megawords of memory and 10 min of CPU time on the Cray Y-MP compared with 30 Megawords and 2 h CPU time required by the exact solution.

Figure 5 shows the parameter domains of validity for each approximation with a specified percentage error for a specular angular region described by $\Delta\theta_{SR}$. The rms roughness to wavelength ratio σ/λ is plotted vs the correlation length to wavelength ratio multiplied by the cosine of the incident angle, $(\tau/\lambda)\cos\theta_0$. The entire region below each line on the graph is the region of validity for the given approximation. The Kirchhoff approximation for an angular region and error criterion is valid for the entire region covered by the Fresnel approximation for the same angular region and energy criterion. Figure 5 shows the parameter domains for typical energy criteria of 90 and 95%, $\mathcal{E}$ < 10 and 5%, within specular angular regions of ±5 and ±10 deg. The Kirchhoff approximation parameter domain does not include the ±5-deg angular region because the criterion is very restrictive.

The angular regions were defined to be ±5 and ±10 deg because these regions are fairly restrictive and provide a significant number of surfaces that are well predicted by both of the engineering approximations. Smaller angular regions significantly reduced the regions for valid predictions by the engineering approximations. Since the approximations are only estimating the scattered energy distribution from a surface, the criteria are broad enough to provide valid results for a significant region of surfaces, yet restrictive enough that the error between the exact predictions and the approximations is small.

The specular approximations work very well when the rms roughness of the surface is small in comparison with the correlation length. Since the approximations are single scattering approximations, they break down when the rms roughness becomes of the order of the correlation length or when retroreflection occurs. This is expected, as the surface is no longer considered optically smooth and more diffuse scattering occurs. Since the Kirchhoff approximation uses the Fresnel relations, the two approximations converge at large correlation lengths. Once the surface roughness to wavelength ratio becomes approximately 2.0, retroreflection occurs for virtually all moderate correlation lengths and the specular approximations fail.

The parameter domains of validity for the approximations in Fig. 5 represent a significant region of random rough surface profiles. All the approximations had to conserve energy and accurately predict the directional distribution of energy for incident angles from θ_0 = 0 to 80 deg in increments of 1 deg. Due to numerical inconsistencies of the exact predictions, the maximum incident angle used is 80 deg. Approximately 100 different cases were compared to make Fig. 5 with correlation length to wavelength ratios ranging from τ/λ = 0.01 to τ/λ = 60.0. The range of rms roughness to wavelength ratios is from σ/λ = 0.0001 to σ/λ = 5.0. In all cases, for both exact and Kirchhoff solutions, approximately 100 surface realizations were used to generate the scattering from the desired surface (specified τ/λ and σ/λ). At correlation lengths smaller than 4.0λ, more cases were compared than at larger surface lengths, because at large correlation lengths the validity of the approximations becomes primarily a function of the rms roughness. Over half of the runs for each approximation were in the region described by τ/λ = 1.0 and τ/λ = 10.0, since this region is the largest region of validity for the Kirchhoff approximation.

As Fig. 5 shows, at moderate correlation length to wavelength ratios of 5.0–20.0, surfaces with significant rms roughness to wavelength ratios of 0.50–1.5 are well approximated as Fresnel surfaces. Although surfaces with roughness to wavelength ratios on the order of σ/λ = 1.0 are not considered optically smooth, the Fresnel engineering approximation predicts the actual angular scattering phenomena within the stated criteria. Likewise, for surfaces as rough as σ/λ = 1.0 with τ/λ = 5.0 at normal incidence, the Kirchhoff approximation can be used to quickly predict the angular distribution of the

energy. For many surfaces with correlation length to wavelength ratios on the order of 1.0, the Kirchhoff approximation provides accurate predictions for roughness to wavelength ratios as large as 0.50. Previously, the Kirchhoff approximation was restricted to $\sigma << \tau$.[13-15] The results presented here extend the region of validity for the Kirchhoff approximation for use in engineering analysis.

Conclusions

The Kirchhoff and Fresnel approximations to the electromagnetic scattering solution can be used to accurately predict angular scattering phenomena from many random rough surfaces of interest. In addition to the conservation of energy criterion, a finite angular criterion based on the region surrounding the specular scattering angle is used to compare the approximations with the exact solution. The specular approximations must conserve energy and predict the angular scattering phenomena. The parameter domains of validity of the approximations are given in Fig. 5, in terms of the surface parameters, roughness and correlation length, and wavelength. The regions of validity of both approximations have been quantified and extended beyond those previously reported. The Fresnel approximation accurately predicts the angular scattering phenomena even when the roughness of the surface is no longer considered optically smooth. The Kirchhoff approximation is also shown to accurately predict the angular phenomena on surfaces in extended ranges of roughness and correlation length. Since the approximations are single scattering solutions of the electromagnetic scattering equations, they are invalid when the roughness of the surface becomes significant in comparison with the correlation length or when retroreflection dominates the exact scattering phenomena.

Using the specular approximations represents a significant reduction in computational time and memory, since the surface matrices in the electromagnetic scattering integrals are not solved. The Kirchhoff approximation reduces the necessary memory by a factor of 100 and the required computational time by a factor of 10 on the Cray Y-MP4/464. The Fresnel approximation is even less computationally expensive than the Kirchhoff approximation. When a reflection distribution is needed, the approximations to the rigorous electromagnetic scattering equations provide a computationally inexpensive solution which accurately predicts the scattering phenomena from many random rough surfaces of interest.

Acknowledgments

This research was supported, in part, by the National Center for Supercomputing Applications, Urbana, Illinois, and the McDonnell Douglas Corporation, St. Louis, Missouri.

References

[1]Wolf, E., "A Generalized Extinction Theorem and Its Role in Scattering Theory," *Coherence and Quantum Optics*, edited by E. Wolf, Plenum Press, New York, 1973, pp. 339–357.

[2]Maradudin, A. A., Michel, T., McGurn, A. R., and Méndez, E. R., "Enhanced Backscattering of Light from a Random Grating," *Annals of Physics*, Vol. 203, No. 2, 1990, pp. 255–307.

[3]Maradudin, A. A., Méndez, E. R., and Michel, T., "Backscattering Effects in the Elastic Scattering of P-Polarized Light from a Large-Amplitude Random Metallic Grating," *Optics Letters*, Vol. 14, No. 3, 1989, pp. 151–153.

[4]Sánchez-Gil, J. A., and Nieto-Vesperinas, M., "Light Scattering from Random Dielectric Surfaces," *Journal of the Optical Society of America A*, Vol. 8, No. 8, 1991, pp. 1270–1286.

[5]Nieto-Vesperinas, M., and Sánchez-Gil, J. A., "Light Scattering from a Random Rough Interface with Total Internal Reflection," *Journal of the Optical Society of America A*, Vol. 9, No. 3, 1992, pp. 424–436.

[6]Celli, V., Maradudin, A. A., Marvin, A. M., and McGurn, A. R., "Some Aspects of Light Scattering from a Randomly Rough Metal Surface," *Journal of the Optical Society of America A*, Vol. 2, No. 12, 1985, pp. 2225–2239.

[7]Beckmann, P., and Spizzichino, A., *The Scattering of Electromagnetic Waves from Rough Surfaces*, Macmillan, New York, 1963, Chap. 3, pp. 17–33.

[8]Davies, H., "The Reflection of Electromagnetic Waves from a Rough Surface," *Proceedings of the IEEE*, Vol. 101, Pt. IV, 1954, pp. 209–214.

[9]Fung, A. K., and Chen, M. F., "Numerical Simulation of Scattering from Simple and Composite Random Surfaces," *Journal of the Optical Society of America A*, Vol. 2, No. 12, 1985, pp. 2274–2284.

[10]Faure-Geors, H., and Maystre, D., "Improvement of the Kirchhoff Approximation for Scattering from Rough Surfaces," *Journal of the Optical Society of America A*, Vol. 6, No. 4, 1989, pp. 532–542.

[11]Kong, J. A., *Electromagnetic Wave Theory*, Wiley, New York, 1990.

[12]Soto-Crespo, J. M., and Nieto-Vesperinas, M., "Electromagnetic Scattering from Very Rough Random Surfaces and Deep Reflection Gratings," *Journal of the Optical Society of America A*, Vol. 6, No. 3, 1989, pp. 367–384.

[13]Chen, M. F., and Fung, A. K., "A Numerical Study of the Regions of Validity of the Kirchhoff and Small-Perturbation Rough Surface Scattering Models," *Radio Science*, Vol. 23, No. 2, 1988, pp. 163–170.

[14]Thorsos, E. I., "The Validity of the Kirchhoff Approximation for Rough Surface Scattering Using a Gaussian Roughness Spectrum," *Journal of the Acoustical Society of America*, Vol. 83, No. 1, 1988, pp. 78–92.

[15]Berman, D. H., and Perkins, J. S., "The Kirchhoff Approximation and First-Order Perturbation Theory for Rough Surface Scattering," *Journal of the Acoustical Society of America*, Vol. 78, No. 3, 1985, pp. 1045–1051.

[16]Siegel, R., and Howell, J. R., *Thermal Radiation Heat Transfer*, Hemisphere, New York, 1981, Chap. 3, p. 64.

[17]Stratton, J. A., *Electromagnetic Theory*, McGraw-Hill, New York, 1941, pp. 23–131.

[18]Brewster, M. Q., *Thermal Radiative Transfer & Properties*, Wiley, New York, 1992, Chaps. 2 and 4.

[19]Morse, P. M., and Feshbach, H., *Methods of Theoretical Physics 1 and 2*, Technology Press, Cambridge, MA, 1946, Chap. 6, p. 155.

[20]Dimenna, R. A., and Buckius, R. O., "Electromagnetic Theory Predictions of the Directional Scattering from Triangular Surfaces," *Journal of Heat Transfer* (to be published).

[21]Abramowitz, M., and Stegun, I. A. (eds.), *Handbook of Mathematical Functions*, Dover, New York, 1965.